Distinct modes of channel gating underlie inactivation of somatic K^+ current in rat hippocampal pyramidal cells *in vitro*

Jean-Louis Bossu * and Beat H. Gähwiler

Brain Research Institute, University of Zurich, August Forel-Strasse 1, CH-8029 Zurich, Switzerland

1. We have used the cell-attached configuration of the patch-clamp recording method to characterize the biophysical properties of the voltage-gated K^+ channel underlying a 4-aminopyridine (4-AP)- and tetraethylammonium (TEA)-sensitive K^+ current ($I_{K(AT)}$) in pyramidal cells of hippocampal slice cultures.

2. The unitary conductance of channels carrying $I_{K(AT)}$ current (K_{AT} channels) was 19·1 ± 5·1 pS with a physiological K^+ gradient (2·7 mM external K^+) and 39·0 ± 3·6 pS with high external K^+ (140 mM). The reversal potential changed with the external K^+ concentration as expected for a channel with a dominant K^+ selectivity. Channel activity was blocked under both conditions by either external application of 4-AP at 100 μM or by including 20 mM TEA in the pipette solution.

3. An analysis of kinetic behaviour showed that open times were distributed as a single exponential. The mean open time (± S.D.) was 4·4 ± 1·4 ms at a voltage 30 mV positive to resting potential and increased with further depolarization to reach a value of 16·2 ± 7·4 ms at 70 mV positive to the resting potential. At this depolarized potential, we observed bursts of channel openings with a mean burst duration around 100 ms.

4. With repeated depolarizing pulses, response failures of the K_{AT} channel occurred in a non-random manner and were grouped (referred to as mode 0). This mode was associated with a voltage-dependent inactivation process of the channel and was favoured when the opening probability of the channel was reduced by increasing steady-state inactivation or by bath application of 4-AP. This is consistent with the localization of the binding site for 4-AP at or near the inactivation gate of the channel.

5. When K_{AT} channel openings were elicited by 500 ms depolarizing steps, activity was either transient or it persisted throughout the duration of the pulse. These two modes of activity alternated in a random manner or occurred in groups giving rise to transient (time constant, 20–100 ms) or sustained ensemble currents. In the presence of low concentrations of 4-AP (20–40 μM), the transient pattern of activity was more frequently observed.

6. In addition to mode 0, we propose the existence of at least two further gating modes for K_{AT} channels: mode T (transient current) and mode S (sustained current) that underlie the three decaying components of the $I_{K(AT)}$ ensemble current. These gating modes are probably under the control of intracellular factors that remain to be identified.

Electrophysiological experiments have revealed the existence of an increasing number of functionally, biophysically and pharmacologically distinct voltage-gated K^+ channels in vertebrate neurones (for review see Rudy, 1988, and for recent single channel data see Forsythe, Linsdell & Stanfield, 1992; Linsdell & Stanfield, 1993). Voltage-gated K^+ channels (K_V channels) are tetramers, each subunit consisting of six transmembrane helices, and belong to a superfamily of ion channel-forming α-polypeptides (Jan & Jan, 1992*a*, 1994). Each subunit is a separate gene product and the functional channel is a homo- or heterotetramer (for reviews see Pongs, 1992; Catterall, 1993). In addition to alternative splicing, gene duplication appears to be a prevalent means for the generation of multiple K^+ channel sequences in mammals. Several genes coding for distinct K^+ polypeptide α-like subunits have been described and

* To whom correspondence should be addressed at the Laboratoire de Neurobiologie Cellulaire, UPR 9009 CNRS Centre de Neurochimie, 5 rue Blaise Pascal, 67087 Strasbourg, France.

grouped into four subfamilies: K_v1, K_v2, K_v3 and K_v4 (Chandy, 1991); a system of classification based on sequence homology assigned to channel classes (*Shaker*, *Shab*, *Shaw* and *Shal*) established for *Drosophila* K^+ channels by Wei, Covarrubias, Butler, Baker, Pak & Salkoff (1990) (for detailed reviews see Jan & Jan, 1992*b*; Pongs, 1992). cDNAs of each subfamily have been expressed in *Xenopus* oocytes enabling the biophysical and pharmacological characterization of each encoded K^+ channel protein.

Rat $K_v2.1$ (or *drk1*; Frech, VanDongen, Schuster, Brown & Joho, 1989) and $K_v2.2$ (or *cdrk*; Hwang, Glatt, Bredt, Yellen & Snyder, 1992), and mouse $K_v2.1$ (Pak, Covarrubias, Ratcliffe & Salkoff, 1991*b*) encode channels mediating both slowly activating and sustained K^+ currents that belong to the delayed rectifier class which are sensitive to tetraethylammonium (TEA). Only rat $K_v2.1$ channels are also 4-aminopyridine (4-AP) sensitive (Pak *et al.* 1991*b*). $K_v4.1$ gives rise to a 4-AP-sensitive (in the millimolar range), TEA-insensitive, fast activating and inactivating K^+ current similar to the A-type K^+ current (I_A) identified in the central nervous system (Baldwin, Tsaur, Lopez, Jan & Jan, 1991; Pak, Baker, Covarrubias, Butler, Ratcliffe & Salkoff, 1991*a*). Several cDNAs that encode proteins belonging to the K_v1 (originally named *RCK*) and K_v3 (originally named *Raw*) gene families and are expressed in the rat brain. Nine proteins for K_v1 ($K_v1.1$ to $K_v1.9$) and four proteins for K_v3 have been recently cloned (for review see Pongs, 1992). Each K_v1 or K_v3 protein assembles into oligomeric voltage-gated K^+ channels with specific functional and pharmacological characteristics. $K_v1.1$ and $K_v1.2$ form non-inactivating channels sensitive to dendrotoxin in the nanomolar range, whereas $K_v1.3$ and $K_v1.4$ channels display similar characteristics as the channels underlying the fast I_A in neurones and are insensitive to TEA but sensitive to 4-AP in the millimolar range (Stühmer *et al.* 1989). $K_v3.1$ and $K_v3.2$ give rise to a delayed rectifier type K^+ current whereas $K_v3.3$ and $K_v3.4$ mediate an A-type K^+ current, both types of current being sensitive to TEA and 4-AP in the millimolar range (Rettig *et al.* 1992; Weiser *et al.* 1994). A further degree of complexity is introduced by the possibility that heteromultimeric K_v channels can be found with biophysical and pharmacological properties which depend upon the precise subunit composition (Ruppersberg, Schröter, Sakmann, Stocker, Sewing & Pongs, 1990; Weiser *et al.* 1994), and also by the recent discovery of a β-subunit controlling the inactivation rate (Rettig *et al.* 1994).

In rat hippocampal pyramidal cells, *in situ* hybridization experiments and Northern blot analysis revealed expression of mRNAs coding for delayed rectifier type K^+ channels, such as $K_v2.2$ (Hwang *et al.* 1992), $K_v1.1$, $K_v1.2$ (Tsaur, Sheng, Lowenstein, Jan & Jan, 1992) $K_v3.1$ and $K_v3.2$ (Weiser *et al.* 1994) and also for A-type K^+ channels, such as $K_v1.4$ (Beckh & Pongs 1990; Sheng, Tsaur, Jan & Jan, 1992; Rettig *et al.* 1992) and $K_v4.2$ (Baldwin *et al.* 1991; Sheng *et al.* 1992; Tsaur *et al.* 1992). Interestingly, K^+ channel proteins display a differential subcellular distribution. $K_v1.2$ and $K_v3.1$ channels are concentrated in the dendritic (Sheng, Tsaur, Jan & Jan, 1994) or axosomatic compartments (Weiser *et al.* 1995), respectively, $K_v1.4$ channels are mainly localized on axons and terminals, and $K_v4.2$ channels are concentrated on somatodendritic membranes (Sheng *et al.* 1992).

In the preceding paper (Bossu, Capogna, Debanne, McKinney & Gähwiler, 1996), we presented evidence that hippocampal pyramidal cells express a dominant K^+ current ($I_{K(AT)}$) at the somatic level exhibiting complex decay kinetics and a high sensitivity to 4-AP in the order of 100 μM, and a sensitivity to TEA in the millimolar range, as well as a small conductance K^+ channel giving rise to an A-type current. More detailed information is needed about the properties of single K^+ channels on native cell membranes in order to be able to establish the role of the various products in determining these macroscopic currents. Here we describe the characteristics of the single channel underlying the $I_{K(AT)}$ ensemble current and propose that it displays distinct channel gating modes giving rise to the multiphasic decay of $I_{K(AT)}$.

METHODS

Hippocampal slices were obtained from 5- to 6-day-old rats (killed by decapitation) and cultured by means of the roller-tube technique as described in the preceding paper (Bossu *et al.* 1996).

The recording chamber was filled with a bath solution at room temperature (at 20 °C) containing: 137 mM NaCl, 2·7 mM KCl, 2·8 mM $CaCl_2$, 2 mM $MgCl_2$, 11·6 mM $NaHCO_3$, 0·4 mM NaH_2PO_4, 5·6 mM glucose, and 5×10^{-7} M tetrodotoxin (TTX) to block propagated electrical activity and reduce transmitter release. The pH was adjusted to 7·4 and monitored with Phenol Red (10 mg ml^{-1}).

Electrophysiological experiments were performed on visually identified CA3 pyramidal cells, using the patch-clamp technique in the cell-attached configuration as described in Bossu *et al.* (1996).

Patch pipettes were filled, for the cell-attached recordings, with the bath solution or with one of the following two solutions (mM): 130 potassium gluconate (or 130 KCl), 10 KCl, 5 Hepes, 2 $MgCl_2$, 2 EGTA, titrated to pH 7·3 with KOH; or 130 KCl, 2·8 $CaCl_2$, 2 $MgCl_2$, 11·6 $NaHCO_3$, 0·4 NaH_2PO_4, 5·6 glucose, titrated with NaOH to pH 7·3.

Single current traces were leak subtracted, using an average formed from episodes that had no channel openings (blank episodes) and scaled appropriately if necessary. The threshold for detecting opening and closing transitions was set at 50% of the open level of each event, rejecting all events that did not exceed 0·5 ms. Data were converted to values corresponding to open times, closed times, and amplitudes. These values provided a way to determine the open probability, the open time and amplitude distributions of the channel. Mean open time of the channel and mean amplitude of unitary currents were obtained by fitting the open time histogram with an exponential function and the amplitude histogram with a Gaussian distribution using the simplex–least-squares fitting method of Clampfit version 6.0.1 (Axon Instruments, Foster City, CA, USA).

Conductance and reversal potential of the channel in single patches were obtained by fitting a linear regression to the mean unitary amplitude values obtained for at least four distinct potentials.

Drugs were applied in the vicinity of the cell by a fast gravity perfusion system (eight-barrelled pipette placed side by side). Drugs were purchased from the following sources: TTX from Sankyo (Tokyo), 4-AP and TEA from Sigma.

Graphs and associated fits were produced using the Fig.P software (version 2.1A; Biosoft, Cambridge, UK). Except where otherwise indicated, results are given as means ± standard deviation.

RESULTS

General observations

A remarkably high density of channels carrying $I_{K(AT)}$ current (K_{AT} channels) was found in cell-attached recordings from the somata of pyramidal cells. It was not possible (except in 1 case out of 154, illustrated in Fig. 6) to record from a patch containing only one channel of this type even when the size of the patch pipette tip was reduced to a minimum. The opening probability of the channels was therefore decreased, in order to facilitate the biophysical analysis of the channels, by tonically depolarizing the patch 10–20 mV. Under these conditions, openings of only two channels could be obtained during prolonged recording periods (about 40 min). The probability of simultaneous opening of both channels (second level openings) was very low and analysis has been confined to first level openings.

Unitary conductance and reversal potential of K_{AT} channels

Figure 1*A* illustrates unitary outward currents evoked with steps of 30, 50 and 60 mV positive to the resting membrane potential (V_r) recorded with a pipette containing 2·7 mM K^+. The opening probability and the amplitude of individual events increased with the magnitude of depolarization. Two channels with identical unitary current amplitude were observed for depolarizations of 50 and 60 mV. The unitary current amplitude has been plotted as a function of the voltage (Fig. 1*C*, open triangles). The current–voltage relationship was linear for potentials between 30 and 90 mV positive to V_r. Linear regression yielded a mean conductance of 19·1 ± 5·1 pS ($n = 14$) and an extrapolated reversal potential of −3·3 ± 9·4 mV ($n = 14$) relative to V_r. The large variability of values for the extrapolated reversal potential could be partly due to variability in the resting potential from cell to cell.

With pipettes containing 140 mM potassium gluconate, unitary inward or outward currents were evoked depending on the step potential applied to the patch. One such patch containing two single channels with similar conductance is illustrated in Fig. 1*B*. Inward currents were elicited with

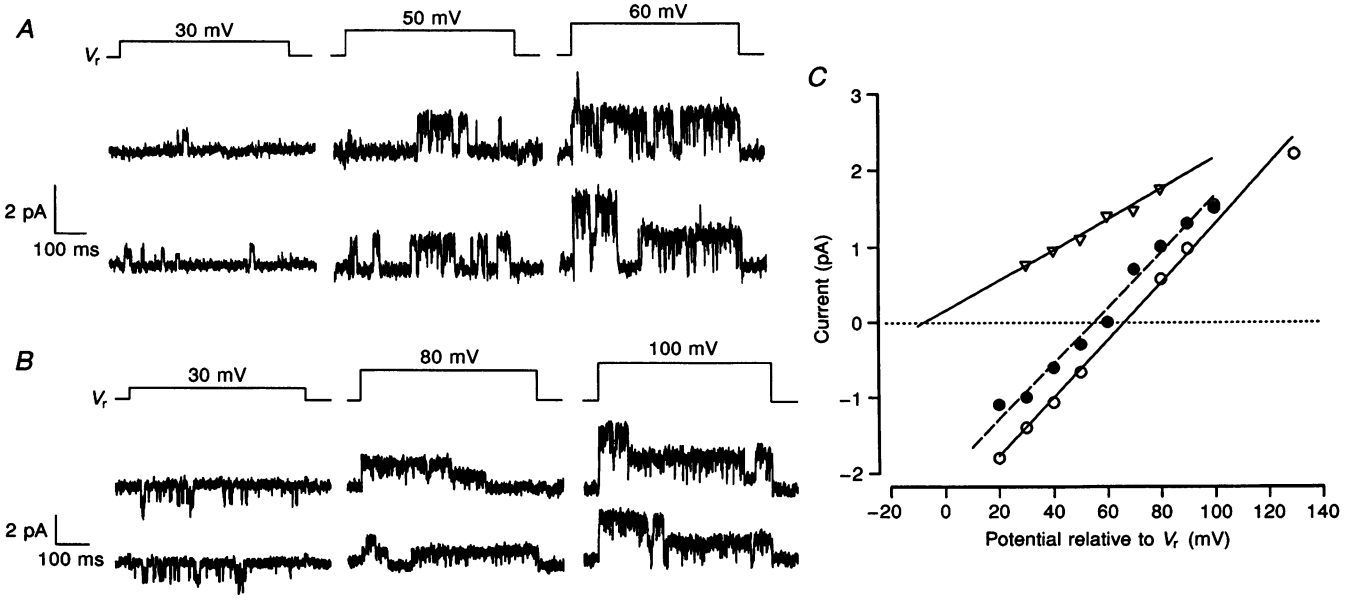

Figure 1. Conductance of the K_{AT} channel

A, unitary $I_{K(AT)}$ recorded with 30, 50 and 60 mV depolarizations from resting potential (V_r). Two channels are present in this patch. *B*, unitary $I_{K(AT)}$ elicited with 30, 80 and 100 mV depolarizations from V_r with a patch pipette containing 130 mM potassium gluconate. Two channels are present. *C*, unitary current–voltage relationships plotting single channel current against membrane potential relative to V_r. For the patch illustrated in *A* (▽), linear regression analysis yields a conductance of 20 pS and an extrapolated reversal potential of −8 mV relative to V_r. The current–voltage relationship for the channels shown in *B* (●) yields a conductance of 37 pS and a reversal potential of 55 mV positive to V_r. The unitary current–voltage relationship for a K_{AT} channel recorded with a patch pipette containing 130 mM KCl (○) yields a conductance of 38 pS and a reversal potential of 65 mV positive to V_r.

depolarizations of 30 mV relative to V_r whereas outward currents were observed for depolarizations of 80 and 100 mV. The current–voltage relationship was linear for potentials between 20 and 100 mV positive to V_r (Fig. 1*C*, filled circles). The mean unitary channel conductance was 39 ± 2 pS ($n = 5$), and the mean reversal potential was 54 ± 2 mV positive to V_r ($n = 5$). The reversal potential and unitary conductance of K_{AT} channels thus depend on the concentration of K^+ in the pipette solution.

When the potassium gluconate-based solution was replaced with KCl, in order to test for the permeability of the channel for Cl^-, the unitary conductance was similar (39 ± 5 pS, $n = 4$); however, the reversal potential was slightly shifted towards a more depolarized potential (62 ± 4 mV, $n = 4$) (Fig. 1*C*, open circles). This shift may reflect differences in the junction potentials produced by the two solutions.

Voltage sensitivity of channel open time

Kinetic analysis of single channel activity was performed at different potentials using pipettes containing 2·7 or 130 mM external K^+. Open time distributions obtained in a single patch for depolarizations of 40 and 60 mV relative to V_r are shown in Fig. 2*A* (2·7 mM external K^+). Regardless of the pipette solution, the distribution was well fitted with a single exponential. The mean open time increased from 4·4 ± 1·4 ms ($n = 8$) for a depolarization of 30 mV, to 16·2 ± 7·4 ms ($n = 13$) for a depolarization of 70 mV relative to V_r (Fig. 2*B*). When recording channel activity with 130 mM external K^+, a similar voltage sensitivity of the mean open times was observed: the open time increased from 4·4 ± 1·8 to 13 ± 4 ms ($n = 4$) for depolarizations of 40 and 70 mV relative to V_r, respectively. Voltage-dependent channel open times have been described for several K^+ channel types. Both the increases of opening probability and of open time with depolarization point to a key role of this channel type in the repolarization of the membrane potential during the action potential (see Bossu *et al.* 1996).

Pharmacological properties of the channel: effects of 4-AP and TEA

External application of 4-AP (100 μM) decreased the opening probability of the channel, when recorded with either a physiological or an isotonic K^+ gradient. The effect of 4-AP occurred with short latency (3–20 s) in both cases and a full blockade was observed after 2–5 min, regardless of whether the channel carried an outward or an inward K^+ current ($n = 8$, data not shown). In the presence of 20 mM TEA in the pipette solution, unitary currents of this type were not elicited by step depolarizations with either K^+ gradient ($n = 10$, data not shown).

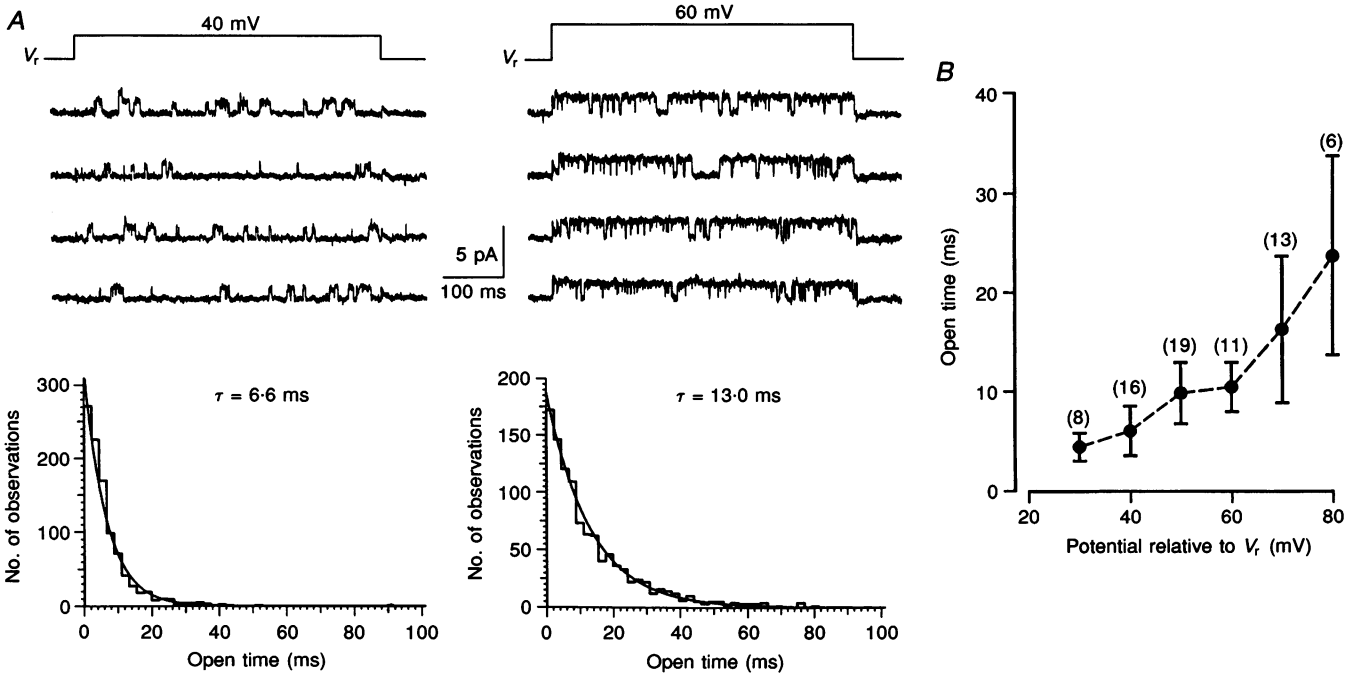

Figure 2. Voltage dependence of K_{AT} channel open times

A: upper panel, unitary currents recorded from a patch depolarized to 40 and 60 mV relative to V_r; lower panel, the corresponding open time histograms, derived from records in which only one channel was open. The frequency distribution of open times is described by a single exponential with a time constant of 6·6 and 13·0 ms at 40 and 60 mV relative to V_r, respectively. *B*, mean open time as a function of the membrane potential relative to V_r. Mean open times were measured from open time histograms such as those shown in *A*. Each point represents a mean value for open times obtained from a number of individual patches, indicated in parentheses, at a given membrane potential. Bars indicate the S.D. of the mean.

Run analysis of channel openings

Mode 0 is associated with a voltage-dependent inactivating process. With repeated depolarizing pulses from resting potential, opening failures tended to occur in groups (Fig. 3*A*). To test whether failures in response to successive sweeps from V_r were significantly grouped, runs of channel openings were counted in a large series of sweeps (N) for patches where the number of sweeps with and without openings were observed in approximately the same proportion. A run is defined as a series of consecutive sweeps in which channel openings occur for each sweep or fail to occur (for a similar analysis see Forsythe *et al.* 1992). If the response to successive voltage pulses is random, the predicted number of runs is $2NP(1 - P)$ where P and $(1 - P)$ are the probabilities for the channel to open or fail to open, respectively. If the observed number of runs is R, one may calculate:

$$Z = (R - 2NP(1 - P))/2\sqrt{NP(1 - P)},$$

(eqn 2.9 from Gibbons, 1971)

where Z is a standardized random variable (mean, 0; S.D., 1). When Z is large and negative, channel openings and

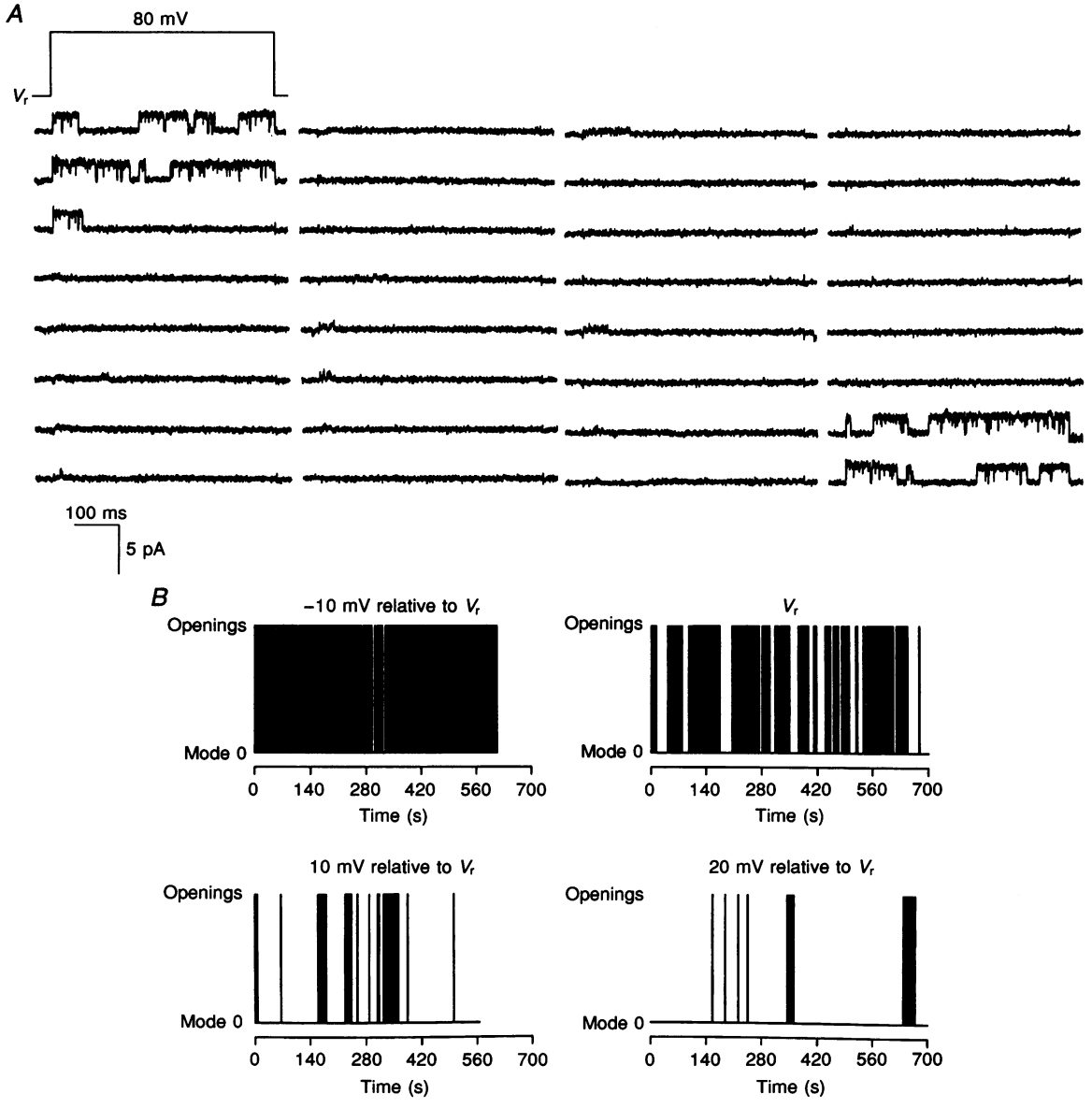

Figure 3. Opening failures of K_{AT} channels during step depolarizations: gating mode 0 is associated with a voltage-dependent inactivation process

A, 32 consecutive current traces (from top to bottom and left to right) in response to repetitive depolarizing voltage pulses (500 ms, every 3 s) from V_r to 80 mV. In this sequence, the channel failed to open during 27 consecutive sweeps. *B*, the occurrence of mode 0 was affected by the holding potential. Diagrams represent the occurrence of mode 0 *versus* channel opening during repetitive 500 ms voltage pulses delivered every 3 s from various holding potentials as indicated above each diagram.

failures in response to successive depolarizing sweeps are significantly grouped. Eight patches were analysed according to this method and a mean Z value of $-3{\cdot}3 \pm 1{\cdot}4$ was obtained. We conclude that the grouping of opening failures was significant under these experimental conditions and therefore constitutes a specific mode of gating that we have named mode 0.

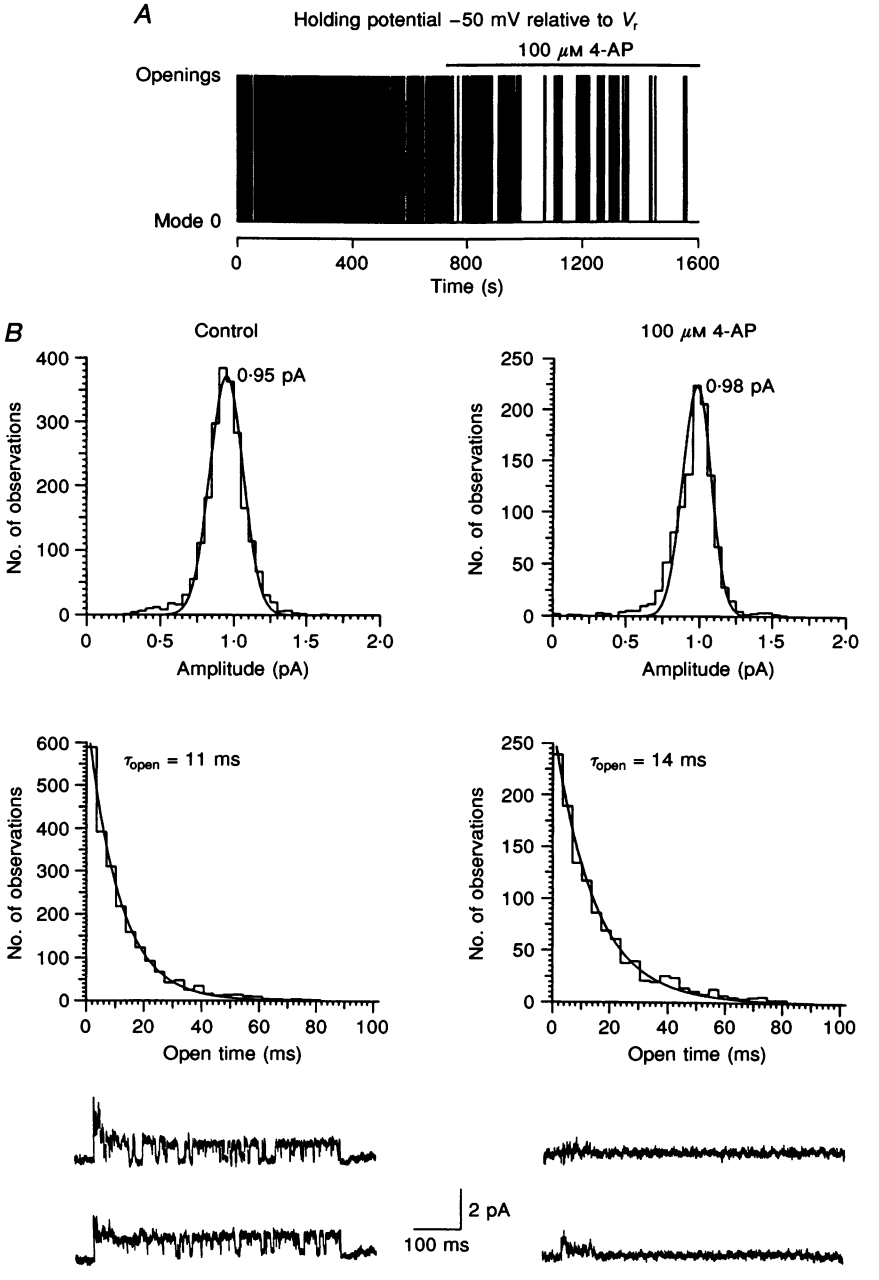

Figure 4. Effect of 4-AP on the occurrence of mode 0

A, diagram illustrating the occurrence of sweeps in which the channel failed to open (mode 0) and sweeps in which the channel did open during repetitive stepping of the patch membrane potential to +50 mV relative to V_r from a holding potential of −50 mV relative to V_r every 3 s. 4-AP (100 μM) was bath applied during the period indicated by the horizontal bar. Note that mode 0 occurred more often in the presence of 4-AP. *B*, same patch as in *A*, amplitude and open time histograms chosen from records where only 1 K_{AT} channel was open before and during application of 4-AP. The unitary current amplitude was 0·95 before and 0·98 pA during application of 4-AP. The open times were distributed according to a single exponential with a time constant (τ_{open}) of 11 ms before and 14 ms in the presence of 4-AP. Lower panel shows 2 consecutive current traces in response to voltage pulses applied from −50 to +50 mV relative to V_r under control conditions (left panel) and during bath application of 4-AP at 100 μM (right panel). Note the presence of small transiently opening channels which are not blocked by 4-AP.

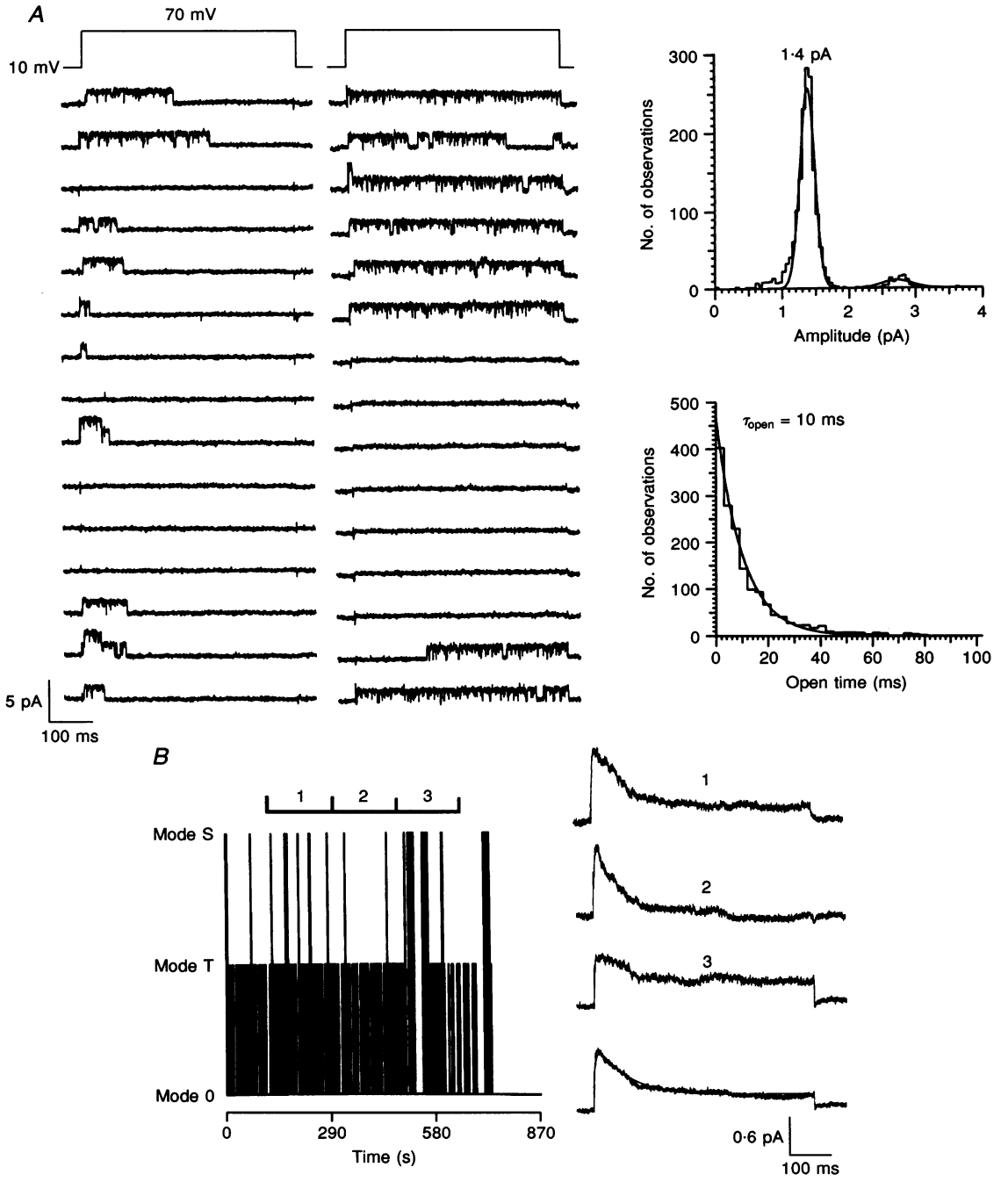

Figure 5. T and S gating modes of the K_{AT} channel: example featuring a dominant T mode

A, the left panel shows 30 consecutive current traces (from top to bottom and left to right) in response to repetitive 500 ms voltage pulses applied every 3 s. During each sweep the patch of membrane was stepped to 70 mV relative to V_r from a holding potential 10 mV positive to V_r. When channel activity was seen, it was either transient (left column) or persisted throughout the sweep (right column). The right panel illustrates the corresponding amplitude and open time histograms. The amplitude histogram revealed 2 unitary current levels, each with an amplitude of 1·4 pA. The open time histogram derived from records where only 1 channel is open has been fitted with a single exponential giving a mean open time of 10 ms. *B*, the left panel shows a diagram representing gating modes based on first level openings. Each sweep was analysed and represented as follows: if the channel failed to open, the sweep was designated mode 0, if the channel opened transiently, it was designated mode T, if channel activity was maintained throughout the sweep, this was designated as mode S. The right panel shows ensemble current traces. Traces 1, 2, 3 represent averages of 60 successive current traces during the corresponding recording periods indicated above the mode diagram shown on the left. The bottom trace represents the ensemble current obtained by averaging all current traces from this recording, with the superimposed line corresponding to the best fit of its decay.

To illustrate the mode history of a channel, data from a large series of consecutive sweeps were graphically represented as minimum (mode 0) and maximum (mode with openings) values (see Fig. 3*B*). The probability of a channel being in mode 0 was a function of holding potential. It increased with depolarizing, and decreased with hyperpolarizing, commands applied to the patch (Fig. 3*B*), showing that mode 0 is associated with a voltage-dependent inactivation process. Groupings of failures to open were also demonstrated in patches containing more than one K_{AT} channel (2–4), suggesting that the channels under the patch were synchronized in the gating mode 0.

If the membrane patch was hyperpolarized by 50 mV, to remove steady-state inactivation of K_{AT} channels, then

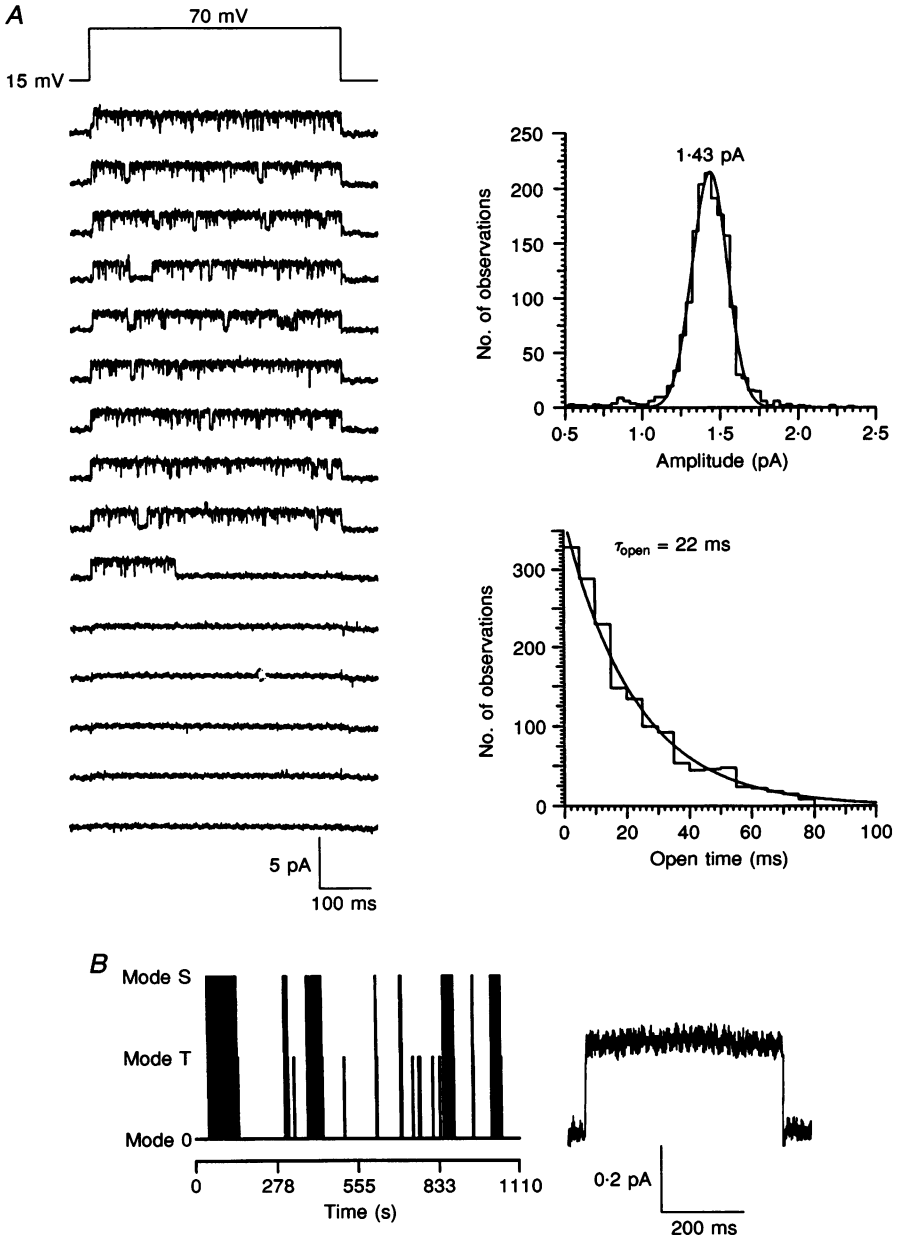

Figure 6. T and S gating modes of the K_{AT} channel: example featuring a dominant S mode

A: left panel, 15 consecutive current traces in response to repetitive 500 ms voltage pulses applied every 3 s. The membrane was stepped to 70 mV relative to V_r from a holding potential 15 mV positive to V_r. During 9 successive sweeps, the channel was in the S mode, then switched to mode T for 1 sweep before entering into mode 0. Right panel, amplitude and open time histograms constructed from this record. This patch contained 1 channel with a current amplitude of 1·43 pA. The open time distribution was fitted by a single exponential with a time constant of 22 ms. *B*: left panel, modes of gating of the K_{AT} channel during all sweeps of the record illustrated in *A*. Note that mode S is dominant. The right panel represents the ensemble current obtained by averaging all current traces displaying channel activity. Note the sustained nature of the ensemble current.

openings were observed in most sweeps. Under these conditions, bath application of 100 μM 4-AP increased the occurrence of mode 0 (Fig. 4*A*). 4-AP affected neither the amplitude (Fig. 4*B*, upper panel) nor the open time (Fig. 4*B*, lower panel) of K_{AT} channels, ruling out a shift to mode 0 through a significant effect of 4-AP on cell membrane potential (similar observations on 4 patches). These data suggest that 4-AP modifies the inactivation process, perhaps by binding to the intracellular portion of the channel.

Modes T and S. K_{AT} channel activity could be observed to either last throughout the duration of the 500 ms depolarization (Fig. 5*A*, left panel, right column) or stop before the end of the pulse (Fig. 5*A*, left panel, left column) in a random or non-random manner depending on the patch and on the recording period in a given patch (data not quantified). Grouping sweeps collected consecutively during extended periods of recording (at least 30 successive steps applied every 3 s, i.e. 114 s) resulted in either transient or sustained ensemble currents. The mean decay time constant of the transient ensemble currents was 47 $\pm$ 24 ms ($n = 16$; range, 18–95 ms). Because these two types of activities can occur in a non-random manner, we suggest that they represent two distinct modes of channel gating. We refer to these as mode T (for transient) for the condition in which channel activity ceases before the end of the 500 ms depolarizing step, and mode S (for sustained), for the condition in which the channels do not inactivate within 500 ms. This duration of 500 ms is >3 times greater than the inactivation time constant of the slow decaying component of $I_{K(AT)}$.

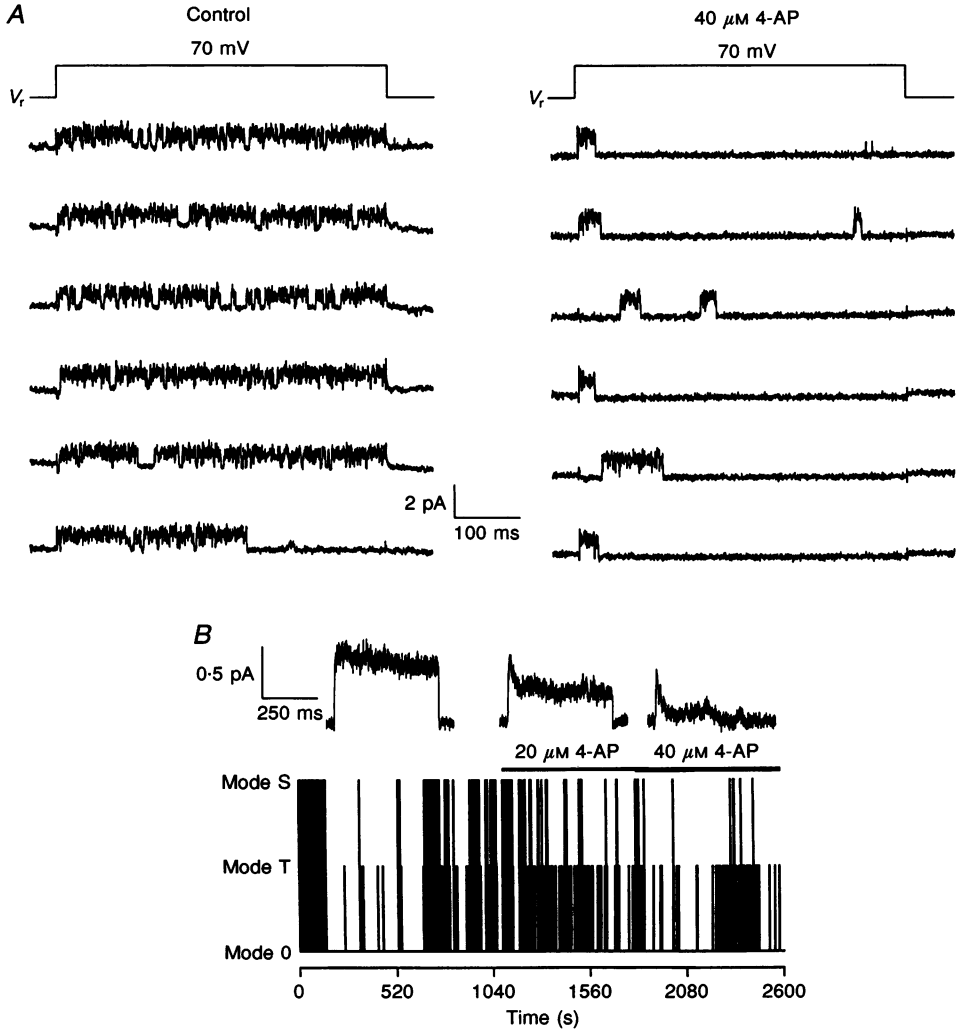

Figure 7. Effects of 4-AP on the gating modes

A, 6 consecutive current traces in response to 70 mV voltage pulses applied from V_r every 3 s under control conditions (left panel) and during bath application of 4-AP at 40 μM (right panel). *B*: lower panel, diagram of gating modes for the full experiment illustrated in *A*. 4-AP was bath applied successively at 20 and 40 μM during the recording periods indicated by the horizontal bars. The current traces in *B* show the ensemble current obtained by averaging all current traces with channel activity during control and 20 and 40 μM 4-AP. This patch has been recorded with 16 mM K^+ in pipette and bath solutions.

Figures 5 and 6 illustrate two patches with K_{AT} channels displaying different behaviour for T and S gating modes. In the example shown in Fig. 5, two K_{AT} channel openings with an amplitude of 1·4 pA and a mean open time of 10 ms were elicited by a depolarization of 70 mV relative to V_r. The opening probability for the first level was 0·085 and for the second level 0·025. The first level had a dominant mode T during some recording periods and then switched to mode S in a non-random manner (Fig. 5*B*, left panel). Averaging recording periods for sixty successive sweeps (Fig. 5*B*, right panel) gave rise to a transient ensemble current with a decay time constant of 51 ms when K_{AT} channel was mainly in mode T (periods 1 and 2) or to a sustained ensemble current when mode S was dominant (period 3). Averaging all sweeps of this recording resulted in an ensemble current with a complex decay including a fast inactivating (time constant, 74 ms) and a sustained component (bottom current trace), as described in the preceding paper (Bossu *et al.* 1996).

The patch illustrated in Fig. 6 contained only one K_{AT} channel activated by the depolarization of 70 mV relative to V_r. The unitary current had an amplitude of 1·4 pA and the channel had an open time of 22 ms (Fig. 6*A*). During periods of activity, the channel opened mainly in the S mode; however, in some sweeps, the channel opened in the T mode (Fig. 6*B*, left panel). In this case, averaging all traces with channel openings produced only a sustained ensemble current (Fig. 6*B*, right panel) because there were so few mode T openings.

Finally, the likelihood for the channel to remain in one mode was examined. In any one patch, mode T openings could occur for single sweeps only, or continuously for 45 min.

4-AP at low concentration favours channel openings in the T mode. The effect of 4-AP on the gating modes of the K_{AT} channel is illustrated in Fig. 7. In this patch, channels opened throughout the duration of the step during most sweeps (Fig. 7*A*, left panel). After bath application of 40 μM 4-AP, the gating behaviour of the channel changed, and channel activity ceased before the end of the step in most sweeps (Fig. 7*A*, right panel). 4-AP at this concentration often increased the latency to the first opening of the channel as well, but this effect was not further quantified. In Fig. 7*B* (lower panel) gating modes of the channel are represented before and during application of two successive concentrations of 4-AP (20 and 40 μM). Under control

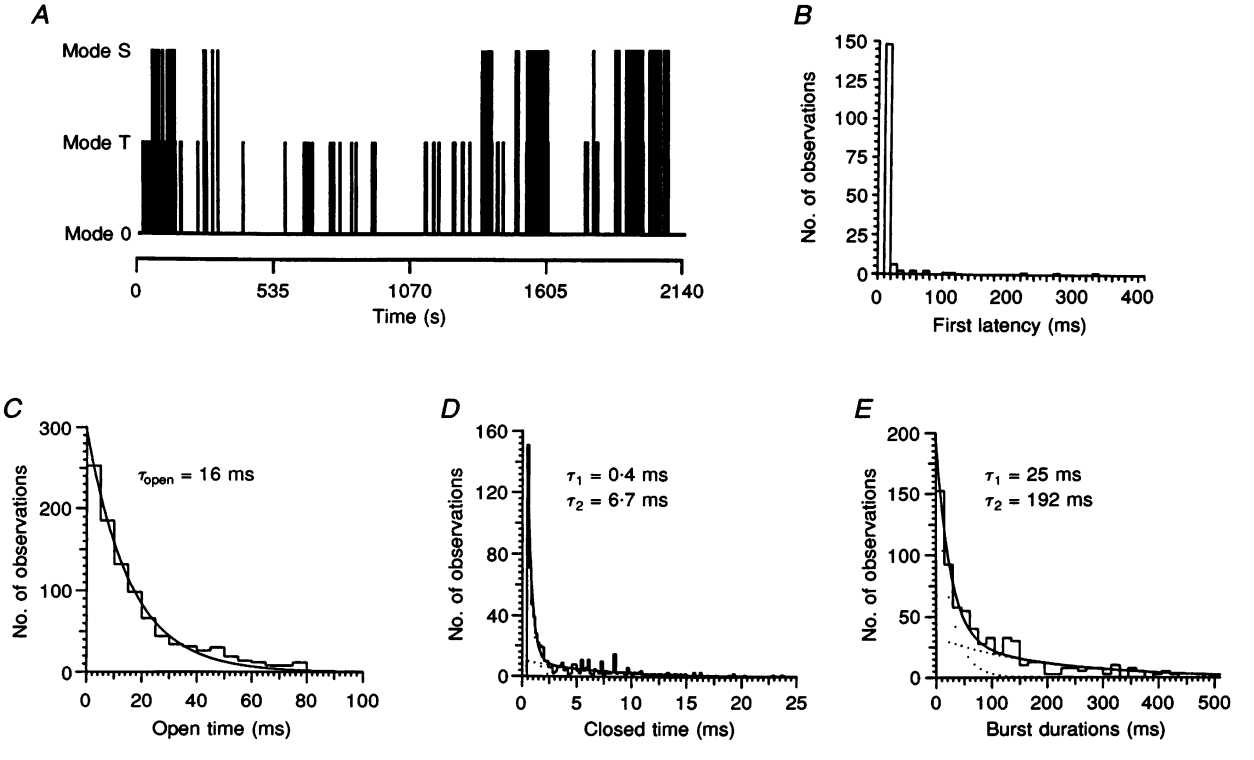

Figure 8. Kinetic properties of the K_{AT} channel determined from a single patch

A, diagram of the gating modes for a patch of membrane depolarized every 3 s to 70 mV relative to V_r from 10 mV positive to V_r. *B* depicts a first latency histogram distribution. First latency was measured from the start of the depolarizing step to the first opening of the channel. *C*, histogram of open times. The continuous (not stepped) line represents a single exponential curve with a time constant of 16 ms. *D*, closed time histogram fitted with two exponentials (continuous line) with time constants of 0·4 and 6·7 ms. *E*, histogram of burst durations. The histogram was fitted with a double exponential (continuous line) with time constants of 25 and 192 ms. Periods of recording exhibiting only one active K_{AT} channel were chosen for determining kinetic parameters.

conditions, when the channel was active during the depolarizing steps, gating was mainly in the S mode giving rise to a sustained ensemble current (Fig. 7*B*, left trace). After application of 20 μM 4-AP, the proportion of sweeps with channel openings in mode T increased, resulting in an ensemble current with transient and sustained components (Fig. 7*B*, middle trace). Increasing the concentration of 4-AP to 40 μM leads to channel gating mainly in the T mode, producing a transient ensemble current decaying with a time constant of 25 ms (Fig. 7*B*, right trace). Similar observations were obtained with three other patches.

Burst analysis

A complete kinetic analysis of K_{AT} channel behaviour was performed from a recording lasting 35 min. During step depolarizations to 70 mV relative to V_r, about the same number of channel openings occurred in the T and S modes (Fig. 8*A*). Upon depolarization, the channel opened with a short latency (in most sweeps between 0·2 and 0·6 ms, Fig. 8*B*) with a mean open time of 16 ms (Fig. 8*C*). The closed time histogram distribution (Fig. 8*D*) has been fitted by the sum of two exponential components, with time constants of 0·4 and 6·7 ms. The fast component was due to very brief closing (flickering) of the channel during bursts. To analyse the distribution of burst durations, we have defined bursts as open events separated by at least 1·5 ms, a value corresponding to about 3 times the fast time constant derived from the closed time histogram distribution. The distribution of burst durations was well fitted with two exponential components having time constants of 25 and 192 ms (Fig. 8*E*). The fast time constant of burst duration (25 ms) thus had a value close to the open time (16 ms).

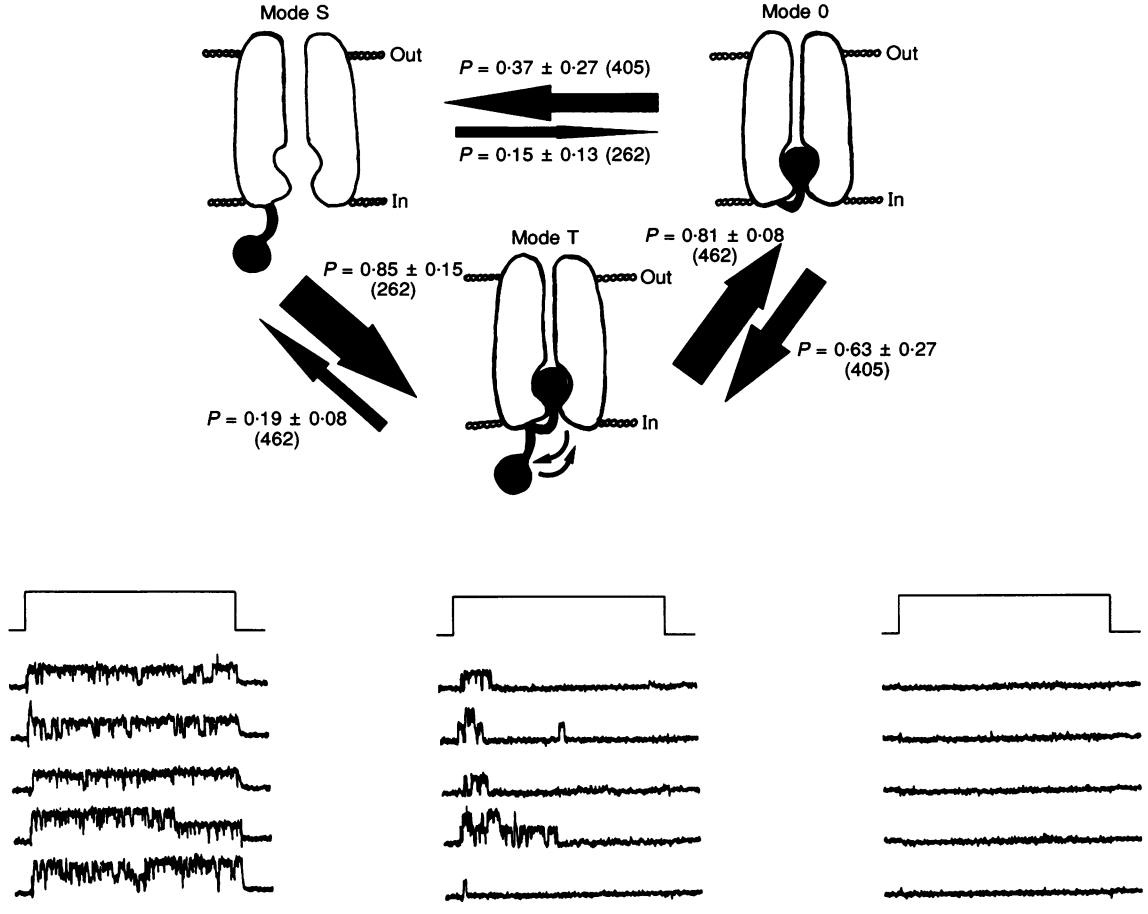

Figure 9. Model of K_{AT} channel gating modes based on different conformations of the inactivation gate

We have considered three distinct modes of gating that we name 0, T, and S. The channel is associated with an intracellular ball and chain-like inactivation gate (in black). This gate can be in three stable configurations: (1) the ball is outside the pore of the channel, a situation underlying gating mode S; (2) the ball blocks the pore with fast onset–offset kinetics, resulting in mode T; and (3) the ball occludes the pore of the channel with slow offset kinetics, leading to gating mode 0. The number above each arrow indicates the probabilities of switching to each of the other two modes after a run in a given mode. The numbers in parentheses indicate the number of runs analysed. Examples of current traces associated with modes S, T and 0 are shown at the bottom (left to right, respectively).

A large number of events is required to validate this type of kinetic analysis. Data were therefore pooled from four recordings during step depolarizations to 70 mV relative to V_r. The unitary current amplitude distribution gave a mean amplitude for the channel of 1·42 pA. As previously shown, the channel usually opened after a very short latency with a single time constant of 20·8 ms. The closed time distribution was fitted by two exponential components, with a time constant of 0·3 and 4·4 ms. The distribution of burst durations followed a biexponential function with time constants of 14·5 and 91 ms. We again observed that the fast time constant of the burst duration was very close to the open time constant.

These observations indicate that K_{AT} channels can in fact open in a non-bursting and a bursting fashion with a mean burst duration in the range 100–200 ms.

Based on the different modes of gating, we can predict that, if the channel is in the T mode during several successive sweeps and opens only once per sweep, (1) it will produce a transient ensemble current, when not bursting, with a decay time constant close to its mean open time (about 25 ms), and (2) it will produce a transient ensemble current, when bursting, with a decay time constant close to the mean duration of bursts (100–200 ms). These predicted values for the decay time constants are close to the time constant of the fast and slowly decaying components of the $I_{K(AT)}$ ensemble current described in the preceding paper (Bossu *et al.* 1996). In the S mode, the channel is always bursting and opens several times during the 500 ms depolarizing step (including single bursts lasting 500 ms), giving rise to the very slowly decaying or sustained component of $I_{K(AT)}$ ensemble current. This indicates that the time course of decay of the macroscopic $I_{K(AT)}$ current depends on at least two parameters: first, on the proportion of bursting *versus* non-bursting K_{AT} channels in the membrane, and second, on the proportion of channels in the T or S mode.

Model of K_{AT} channel gating modes

The model illustrated in Fig. 9 represents our working hypothesis. We propose the existence of three gating modes for the K_{AT} channel (S, T and 0) that correspond to distinct conformations of the inactivation gate. This gate is depicted as the inactivating ball peptide described for several cloned K^+ channels (for review see Jan & Jan, 1992*b*, 1994). According to this model, a cytoplasmic gate intrinsic to the channel (the ball) binds to the cytoplasmic mouth of the pore after the channel opens, thereby occluding the pore. The mode S corresponds to the period of time when the channel is not inactivated by the ball. In mode T, the ball blocks the pore of the channel with fast onset and offset kinetics. In mode 0, the ball occludes the channel for long periods. Bursting behaviour of the channel may correspond to a blocking action of the ball with a very fast onset and offset occurring when the channel is in the S or T mode (not represented in this model).

Following a run in a given gating mode, analysis of the probability for the channel entering one of the other gating modes reveals that after a run in the S mode the channel switches with a high probability to mode T (0·85), and after a run in the T mode the channel switches with a high probability to the 0 mode (0·81). After a run in the 0 mode the channel switches with a high probability either into the T or the S mode depending on the patch (this explains the large standard deviation of the mean transition probabilities).

4-AP (10–40 μM) shifts the equilibrium between gating modes towards the T mode, and, at higher concentrations, towards the 0 mode. This suggests a dose-dependent action of 4-AP in setting the conformation of the inactivating gate of the K_{AT} channel.

DISCUSSION

We have characterized the channel underlying the 4-AP- and TEA-sensitive ($I_{K(AT)}$) ensemble current at the somatic level of hippocampal pyramidal cells described in the preceding paper (Bossu *et al.* 1996). The data of the present paper could be described either by the presence of several channel subtypes with similar single channel conductances, or alternatively by a single channel operating in different gating modes. Although our data do not allow us to distinguish unambiguously between these two possibilities, we favour the latter hypothesis because the unitary conductance of channels exhibiting S and T gating were identical in both physiological and symmetrical K^+ gradients and because channel open time could be described by a single voltage-dependent process. In addition, when two channels were activated in a given patch, they could open simultaneously either in the T or S mode. Furthermore, the single channel open times and the burst durations corresponded well to the kinetics of the ensemble currents. Finally, the grouping of the two gating modes and the distinct probabilities of switching between the different modes are more easily explained by assuming a single channel type with different gating modes than the presence of two distinct and independent channels. For example, if two channel types were present, then the opening of one channel type would have to preclude the opening of the other type.

The amplitude and the time course of the decay of the ensemble current thus depends on the proportion of K_{AT} channels gating in a particular mode in the patch. A similar interpretation has been proposed to explain the complex decay kinetics of I_A in sensory neurones (Cooper & Shrier, 1989) and the fast and slow inactivation of Na^+ channels in rat and heart muscle (Patlak & Ortiz, 1986). Furthermore, depending on the patch, the channel can open in one dominant mode, but also can switch to another mode for long periods of time. This suggests that intracellular factors may play a role in the control of K_{AT} channel gating modes.

Mode 0 is associated with a voltage-dependent inactivation process

Clustering of sweeps without activity has been described for most voltage-gated channels including Na^+ channels (Horn, Vandenberg & Lange, 1984), Ca^{2+} channels (Hess, Lansman & Tsien, 1984), A-type K^+ channels (Cooper & Shrier, 1989; Forsythe *et al.* 1992) and delayed rectifier K^+ channels (Rogawski, 1986; Hoshi & Aldrich, 1988). Adopting the terminology proposed by Hess *et al.* (1984) for the L-type Ca^{2+} channel, we have interpreted absence of activity as a mode of gating called mode 0.

Since voltage-dependent inactivation is one factor that increased the proportion of time a channel spent in mode 0, we associate this mode of gating with a series of slow steps involved in the inactivation process (see Forsythe *et al.* 1992 for a similar conclusion). This suggests the presence of a conformational change in the channel protein where a peptide 'ball' occludes the pore with a very slow offset. This inactivated conformation of the channel could be very stable, lasting more than 15 min. From a physiological point of view, two observations concerning mode 0 are important: first, long periods of mode 0 were observed when the channel was recorded at resting potential, and second, when many channels were localized under the patch they were usually synchronized in mode 0. It is conceivable that, at the resting membrane potential, cells can shift into periods of increased excitability where K_{AT} channels gate in mode 0 in a synchronized manner.

As with dihydropyridine antagonists acting on L-type Ca^{2+} channels (Hess *et al.* 1984), 4-AP at 100 μM stabilized the channel in mode 0, with no evidence for a change in the current amplitude and open time distribution. Similar effects of 4-AP have been observed at the single channel level for cloned K^+ channels such as *Shaker* 29–4 (McCormack, Joiner & Heinemann, 1994) and $K_v1.4$ (Yao & Tseng, 1994). Based on our model, 4-AP should stabilize the binding of the ball within the mouth of the channel. Consistent with this idea, recent experiments on mouse $K_v1.1$ channels indicate that 4-AP acts intracellularly at or near the binding site for the inactivation peptide (Stephens, Garratt, Robertson & Owen, 1994).

Modes T and S control the decay kinetics of $I_{K(AT)}$

Mode T refers to the condition where channel activity terminates before the end of the 500 ms depolarizing step, and mode S the condition where the channel does not inactivate during a 500 ms pulse. During extended recording periods, the stability of such gating modes varied not only from patch to patch, but also during the time of recording for a given patch, with cycling of activity between mode S and T being observed. Depending on the characteristics of these cycles, sustained or transient ensemble currents could be generated. A similar gating behaviour has been demonstrated for the N-type Ca^{2+} channel by Plummer & Hess (1991) and has been interpreted as a reversible uncoupling of inactivation.

During periods in mode T, the decay kinetics of the ensemble current varied from cycle to cycle, or from one patch to another, with time constant values ranging between 18 and 95 ms, reflecting channel activity during periods of non-bursting or bursting behaviour, respectively (see Rogawski, 1986 and Linsdell & Stanfield, 1993 for similar analysis of bursts with the hippocampal delayed rectifier K^+ channel).

For our model, we propose that mode T is linked to the inactivation gate, which occludes the channel with fast onset–offset kinetics. We assume that mode T and mode 0 result from conformational changes of this same gate. Two main observations support this hypothesis: first, after a run in mode T, the channel switched to mode 0 with a higher probability then to mode S, and second, mode T and mode 0 were both stabilized by 4-AP but at different concentrations. In contrast to our observations on mode 0, however, we have no evidence for a dependence of mode T on steady-state inactivation (data not illustrated).

During periods in mode S, the interaction of the pore region and the ball peptide is prevented, perhaps because of covalent modification of the channel as proposed by Plummer & Hess (1991) for the N-type Ca^{2+} channel.

Factors controlling gating modes

An important issue will be to determine the external or internal factors controlling the stability of K_{AT} channels in the different gating modes. Intracellular compounds that reduce or oxidize cysteine residues are good candidates. Indeed, it has been shown that such compounds control the inactivation behaviour of the A-type K^+ channels by regulating the formation of disulphide bridges between the ball domain and a part of the channel protein (Ruppersberg, Stocker, Pongs, Heinemann, Frank & Koenen, 1991). Phosphorylation and dephosphorylation processes must also be considered. For example, Wilson & Kaczmarek (1993) demonstrated a switch in gating mode for a voltage-gated cation channel triggered by a protein kinase A-regulated, tyrosine phosphatase.

Comparison with cloned voltage-gated K^+ channels

K_v3 channel proteins display a sensitivity to TEA and 4-AP in a concentration range similar to K_{AT} channels. They induce, however, currents with kinetics that differ from $I_{K(AT)}$ ensemble currents. $K_v3.1$ and $K_v3.2$ generate non-inactivating, delayed rectifier type K^+ currents, whereas $K_v3.3$ produces a fast inactivating current. At the single channel level, the conductance measured for $K_v3.1$ is very close to the conductance for $I_{K(AT)}$ (for review see Pongs, 1992). The channel we described could result from the heteromultimeric assembly of $K_v3.1$ and $K_v3.3$ proteins including the ball and chain inactivation gate. Another interesting alternative published recently by Rettig *et al.* (1994) proposes that the association of a β-subunit, present in the rat nervous system, confers rapid A-type inactivation to delayed rectifier type K^+ channels. Furthermore, the

gating mode giving rise to the complex decay kinetics of $I_{K(AT)}$ could result from the binding and unbinding properties of such β-subunits to delayed type channel proteins from the K_v3 family. Finally, we cannot exclude the presence of two distinct mechanisms of inactivation, a rapid inactivation (N-type) link to the ball–chain and a much slower inactivation process (C-type). The switch from S to T modes may then correspond to a suppression of the C-type inactivation. Accordingly, C-type inactivation has been shown to be influenced by cytoplasmic factors (Marom, Goldstein, Kupper & Levitan, 1993) via some interaction between extracellular and intracellular amino acids in regulating channel function (Kupper, Bowlby, Marom & Levitan, 1995). A molecular characterization of the channel underlying $I_{K(AT)}$ will be required to differentiate between these hypotheses.

Baldwin, T. J., Tsaur, M. L., Lopez, G. A., Jan, Y. N. & Jan, L. Y. (1991). Characterization of a mammalian cDNA for an inactivating voltage-sensitive K^+ channel. *Neuron* **7**, 471–483.

Beckh, S. & Pongs, O. (1990). Members of RCK potassium channel family are differentially expressed in the rat nervous system. *EMBO Journal* **9**, 777–782.

Bossu, J.-L., Capogna, M., Debanne, D., McKinney, R. A. & Gähwiler, B. H. (1996). Somatic voltage-gated potassium currents of rat hippocampal pyramidal cells in organotypic slice cultures. *Journal of Physiology* **495**, 367–381.

Catterall, W. A. (1993). Structure and function of voltage-gated ion channels. *Trends in Neurosciences* **16**, 500–506.

Chandy, K. G. (1991). Simplified gene nomenclature. *Nature* **352**, 26.

Cooper, E. & Shrier, A. (1989). Inactivation of A currents and A channels on rat nodose neurons in culture. *Journal of General Physiology* **94**, 881–910.

Forsythe, I. D., Linsdell, P. & Stanfield, P. R. (1992). Unitary A-currents of rat locus coeruleus neurones grown in cell culture: rectification caused by internal Mg^{2+} and Na^+. *Journal of Physiology* **451**, 553–583.

Frech, G. C., VanDongen, A. M. J., Schuster, G., Brown, A. M. & Joho, R. H. (1989). A novel potassium channel with delayed rectifier properties isolated from brain by expression cloning. *Nature* **340**, 642–645.

Gibbons, J. D. (1971). *Nonparametric Statistical Interference*. McGraw–Hill, New York.

Hess, P., Lansman, J. B. & Tsien, R. W. (1984). Different modes of Ca channel gating behaviour favoured by dihydropyridine Ca agonists and antagonists. *Nature* **311**, 538–544.

Horn, R., Vandenberg, C. A. & Lange, K. (1984). Statistical analysis of single sodium channels. Effects of N-bromoacetamide. *Biophysical Journal* **45**, 323–335.

Hoshi, T. & Aldrich, R. W. (1988). Gating kinetics of four classes of voltage-dependent K^+ channels in pheochromocytoma cells. *Journal of General Physiology* **91**, 107–131.

Hwang, P. M., Glatt, C. E., Bredt, D. S., Yellen, G. & Snyder, S. H. (1992). A novel K^+ channel with unique localizations in mammalian brain: molecular cloning and characterization. *Neuron* **8**, 473–481.

Jan, L. Y. & Jan, Y. N. (1992*a*). Tracing the roots of ion channels. *Cell* **69**, 715–718.

Jan, L. Y. & Jan, Y. N. (1992*b*). Structural elements involved in specific K^+ channel functions. *Annual Review of Physiology* **54**, 537–555.

Jan, L. Y. & Jan, Y. N. (1994). Potassium channels and their evolving gates. *Nature* **371**, 119–122.

Kupper, J., Bowlby, M. R., Marom, S. & Levitan, I. B. (1995). Intracellular and extracellular amino acids that influence C-type inactivation and its modulation in voltage-dependent potassium channel. *Pflügers Archiv* **430**, 1–11.

Linsdell, P. & Stanfield, P. R. (1993). Unitary delayed rectifier channels of rat hippocampal neurons: properties of block by external tetraethylammonium ions. *Pflügers Archiv* **425**, 41–53.

McCormack, K., Joiner, W. J. & Heinemann, S. H. (1994). A characterization of the activating structural rearrangements in voltage-dependent *Shaker* K^+ channels. *Neuron* **12**, 301–315.

Marom, S., Goldstein, S. A., Kupper, J. & Levitan, I. B. (1993). Mechanism and modulation of inactivation of the Kv3 potassium channel. *Receptors and Channels* **1**, 81–88.

Pak, M. D., Baker, K., Covarrubias, M., Butler, A., Ratcliffe, A. & Salkoff, L. (1991*a*). mShal, a subfamily of A-type K^+ channel cloned from mammalian brain. *Proceedings of the National Academy of Sciences of the USA* **88**, 4386–4390.

Pak, M. D., Covarrubias, A., Ratcliffe, A. & Salkoff, L. (1991*b*). A mouse brain homolog of the *drosophila* Shab K^+ channel with conserved delayed-rectifier properties. *Journal of Neuroscience* **11**, 869–880.

Patlak, J. B. & Ortiz, M. (1986). Two modes of gating during late Na^+ channel currents in frog sartorius muscle. *Journal of General Physiology* **87**, 305–326.

Plummer, M. R. & Hess, P. (1991). Reversible uncoupling of inactivation in N-type calcium channels. *Nature* **351**, 657–659.

Pongs, O. (1992). Molecular biology of voltage-dependent potassium channels. *Physiological Reviews* **72**, S69–88.

Rettig, J., Heinemann, S. H., Wunder, F., Lorra, C., Parcej, D. N., Dolly, J. O. & Pongs, O. (1994). Inactivation properties of voltage-gated K^+ channels altered by presence of β-subunit. *Nature* **369**, 289–294.

Rettig, J., Wunder, F., Stocker, M., Lichtinghagen, R., Mastiaux, F., Beckh, S., Kues, W., Pedarzani, P., Schröter, K. H., Ruppersberg, J. P., Veh, R. & Pongs, O. (1992). Characterization of a Shaw-related potassium channel family in rat brain. *EMBO Journal* **11**, 2473–2486.

Rogawski, M. A. (1986). Single voltage-dependent potassium channels in cultured rat hippocampal neurons. *Journal of Neurophysiology* **56**, 481–493.

Rudy, B. (1988). Diversity and ubiquity of K channels. *Neuroscience* **25**, 729–749.

Ruppersberg, J. P., Schröter, K. H., Sakmann, B., Stocker, M., Sewing, S. & Pongs, O. (1990). Heteromultimeric channels formed by rat brain potassium-channel proteins. *Nature* **345**, 535–537.

Ruppersberg, J. P., Stocker, M., Pongs, O., Heinemann, S. H., Frank, R. & Koenen, M. (1991). Regulation of fast inactivation of cloned mammalian IK(A) channels by cysteine oxydation. *Nature* **352**, 711–714.

Sheng, M., Tsaur, M. L., Jan, Y. N. & Jan, L. Y. (1992). Subcellular segregation of two A-type K^+ channel proteins in rat central neurons. *Neuron* **9**, 271–284.

SHENG, M., TSAUR, M. L., JAN, Y. N. & JAN, L. Y. (1994). Contrasting subcellular localization of the Kv1.2 K^+ channel subunit in different neurons of rat brain. *Journal of Neuroscience* **14**, 2408–2417.

STEPHENS, G. J., GARRATT, J. C., ROBERTSON, B. & OWEN, D. G. (1994). On the mechanism of 4-aminopyridine action on the cloned mouse brain potassium channel mKv1.1. *Journal of Physiology* **477**, 187–196.

STÜHMER, W., RUPPERSBERG, J. P., SCHRÖTER, K. H., SAKMANN, B., STOCKER, M., GIESE, K. P., PERSCHKE, A., BAUMANN, A. & PONGS, O. (1989). Molecular basis of functional diversity of voltage-gated potassium channels in mammalian brain. *EMBO Journal* **8**, 3235–3244.

TSAUR, M. L., SHENG, M., LOWENSTEIN, D. H., JAN, Y. N. & JAN, L. Y. (1992). Differential expression of K^+ channel mRNAs in the rat brain and downregulation in the hippocampus following seizures. *Neuron* **8**, 1055–1067.

WEI, A., COVARRUBIAS, M., BUTLER, A., BAKER, K., PAK, M. & SALKOFF, L. (1990). K^+ current diversity is produced by an extended gene family conserved in *Drosophila* and mouse. *Science* **248**, 599–603.

WEISER, M., BUENO, E., SEKIRNJAK, C., MARTONE, M. E., BAKER, H., HILLMAN, D., CHEN, S., THORNHILL, W., ELLISMAN, E. & RUDY, B. (1995). The potassium channel subunit KV3.1b is localized to somatic and axonal membranes of specific populations of CNS neurons. *Journal of Neuroscience* **15**, 4298–4314.

WEISER, M., VEGA-SAENZ DE MIERA, E., KENTROS, C., MOREMO, H., FRANZEN, L., HILLMANN, D., BAKER, H. & RUDY, B. (1994). Differential expression of *Shaw*-related K^+ channels in the rat central nervous system. *Journal of Neuroscience* **14**, 949–972.

WILSON, G. F. & KACZMAREK, L. K. (1993). Mode-switching of a voltage-gated cation channel is mediated by a protein kinase A-regulated tyrosine phosphatase. *Nature* **366**, 433–438.

YAO, J. A. & TSENG, G. N. (1994). Modulation of 4-AP block of a mammalian A-type K channel clone by channel gating and membrane voltage. *Biophysical Journal* **67**, 130–142.

Acknowledgements

The authors are indebted to Professor O. Pongs, Drs U. Gerber and S. M. Thompson for constructive criticism and reading the manuscript. We also thank L. Rietschin and L. Heeb for preparing and feeding the cultures, E. Hochreutener for the design of figures and R. Schöb for photographic work. This work was supported by the Roche Research Foundation, the European Economic Community (grant no. ERBCHBICT941256) and the Swiss National Science Fundation (31-42174.94).

Author's email address

J.-L. Bossu: jlbossu@neurochem.u-strabg.fr

Received 24 August 1995; accepted 7 May 1996.